Low-energy trajectories from geosynchronous transfer orbits to lunar libration orbits

Pascarella, Alex; Noomen, Ron; Wilson, Roby

Publication date
2021

Document Version
Accepted author manuscript

Published in
ASTRODYNAMICS 2020

(Preprint) AAS 20-693

LOW-ENERGY TRAJECTORIES FROM GEOSYNCHRONOUS TRANSFER ORBITS TO LUNAR LIBRATION ORBITS

Alex Pascarella[*], Ron Noomen[†], and Roby Wilson[‡]

The ability to reduce the cost of space missions beyond Earth orbit by leveraging innovative concepts is of great interest in the field of spaceflight. In this paper, the trajectory design for a mission from an inclined geosynchronous transfer orbit (GTO) to an Earth-Moon L2 Halo orbit is presented. The mission scenario for this investigation involves the use of a small satellite launched in a rideshare configuration and the use of a low-energy transfer to reach the target orbit. As a consequence of choosing a rideshare launch, the mission scenario entails critical uncertainties on the time of launch and injection parameters of the spacecraft, which could complicate the insertion into a low-energy transfer. Thus, the goal of the project is to develop a robust design methodology to deal with the launch uncertainties and assess launch readiness at any time of the year.

INTRODUCTION

The focus of this paper is the analysis of low-energy trajectories to Earth-Moon libration orbits for small satellites launched in a rideshare configuration.

Rideshare launches are a convenient option to reduce the launch cost of small satellite missions. For missions in the Earth-Moon system, rideshares to GTO prove to be especially useful, because they allow for several launch opportunities throughout the year and they provide a much larger semimajor axis (i.e. energy state) than a launch into low earth orbit (LEO). Comparison of the results presented in Pernicka[1] and Genova[2] shows a drastic reduction in the ΔV requirements when injecting into a low-energy transfer to the Moon from GTO rather than LEO.

In the Earth-Moon environment, low-energy trajectories are made possible by the interaction of the invariant manifolds of the Sun-Earth system and of the Earth-Moon system,[3] which yields trajectories with a lower ΔV but a longer time of flight than a direct, Hohmann-like transfer. Low-energy transfers in the Earth-Moon system have been studied for a long time, with particular interest in trajectories from LEO to the Moon as a more fuel-efficient solution than a direct transfer.[4]

Previous work that analyzes low-energy trajectories starting from GTO includes studies of trajectories from GTO to Sun-Earth libration orbits,[5] trajectories from GTO to the Moon using either the Earth-Moon invariant manifolds[6] or the Sun-Earth and Earth-Moon invariant manifolds,[2,7] as well as trajectories from GTO to Earth-Moon L1 Halo orbits leveraging invariant manifolds and low-thrust propulsion.[8,9]

[*]Master student, Faculty of Aerospace Engineering, Delft University of Technology, Kluyverweg 1, 2629 HS Delft, the Netherlands.

[†]Assistant professor, Faculty of Aerospace Engineering, Delft University of Technology, Kluyverweg 1, 2629 HS Delft, the Netherlands.

[‡]Technical group supervisor, Jet Propulsion Laboratory, California Institute of Technology, Pasadena, 91109, USA

The present investigation assumes a launch from the Cape Canaveral Eastern Test Range into a 185 by 35786 km altitude GTO at an inclination of 28.5°. A methodology based on impulsive maneuvers and two-body dynamics is used to compute the maneuvers required to move the spacecraft from its initial orbit into a low-energy transfer to a northern Halo orbit around the Earth-Moon L2 point. In order to provide a broad picture of the problem, the analysis covers the epochs for the year 2022.

BACKGROUND

For this mission scenario, it is assumed that the spacecraft is integrated in an EELV Secondary Payload Adapter (ESPA) and launched in a GTO at an inclination of 28.5° and argument of periapsis of 180°, which is compatible with a launch from Cape Canaveral. It is assumed that the wet mass of the spacecraft is 180 kg (in compliance with the ESPA mass requirements), the propellant mass is 90 kg and the I_{sp} is 300 s: taken together, this yields a maximum ΔV budget of 2.04 km/s. The mean solar time at periapsis of the GTO is not known a priori but is dictated by the primary payload of the rideshare launch.

The software used for the trajectory design is the Mission Analysis, Operations, and Navigation Toolkit Environment (MONTE) developed by JPL.[10] The candidate orbit for the mission was selected from a database of Earth-Moon libration orbits, which is also available within the MONTE library.

The target orbit selected for this investigation is a northern Halo orbit around the Earth-Moon L2 point with a period of approximately 15 days. The circular restricted three-body (CR3BP) model is leveraged in the preliminary design of transfer trajectories in the Earth-Moon system. The CR3BP is defined in a frame corotating with two primary bodies of mass m_1 and m_2 and centered at the barycenter of the system. The equations of motion of the CR3BP are given by[11]

$$\ddot{x} - 2\dot{y} = U_x \tag{1a}$$

$$\ddot{y} + 2\dot{x} = U_y \tag{1b}$$

$$\ddot{z} = U_z \tag{1c}$$

The potential is expressed as $U = \frac{1-\mu}{r_1} + \frac{\mu}{r_2} + \frac{1}{2}(x+y)$, where r_1 and r_2 are the distances between the body and the primaries and $\mu = \frac{m_2}{m_1+m_2}$ is the mass parameter of the system.

The CR3BP model is used to specify the target libration orbit for the mission, whose state in the rotating frame is stored in the orbit database available in MONTE. Transfers to an unstable periodic orbit can be found by computing its stable manifold, which corresponds to the set of trajectories that converge to the periodic orbit itself. The stable manifold is found by computing the eigenvalues of the monodromy matrix,[3] which is the state transition matrix (STM) after one revolution of the periodic orbit. By carrying out this computation for different points along the orbit, a large number of dynamical states belonging to the stable manifold are obtained. These states are then propagated backward in time (either using the patched three-body model or a more accurate dynamical model, such as the ephemeris model) until a suitable trajectory is found. In particular, for the Sun-perturbed Earth-Moon system, it can be observed that the invariant manifolds of the Earth-Moon system interact with the invariant manifolds of the Sun-Earth system in such a way that fuel-efficient transfer

trajectories from Earth to the Moon vicinity can be found.[12] To show the behavior of the dynamical system, it is common to represent the trajectories using the Sun-Earth and Earth-Moon rotating frames.

Despite using the CR3BP to generate the dynamical states lying on the stable manifold of the Earth-Moon libration orbit, the actual dynamical model used for the trajectory propagation is an ephemeris model that incorporates the point mass gravity of the major bodies of the Solar System, whose positions as a function of time are supplied by the JPL DE430 ephemeris. Since the ephemeris model is a high-fidelity representation of the dynamics of the Solar System, it is not required to transition the trajectories to a more accurate model.

During the initial phase of the trajectory, when the spacecraft is close to the Earth, the dynamical model also includes the effect of the atmospheric drag, described by the DTM model,[13] and the effect of the Earth's spherical harmonics, described by the EGM96 model truncated at degree and order 4. Furthermore, all orbital maneuvers are assumed to be impulsive, so that the required propellant mass can be estimated from Tsiolkovsky's equation $\Delta V = -g_o \, I_{sp} \ln \dfrac{m_f}{m_0}$.

DESIGN METHODOLOGY

Transfer Trajectory Design

Following the methodology proposed by Parker,[12] the transfers to the target orbit are found by computing the stable manifold of the orbit for different arrival epochs and propagating its states backward in time until a periapsis near Earth is found or the maximum propagation time is reached. The stepsize of the arrival epochs and the stepsize for the generation of the manifold are both set to 3 hours, in order to generate a large quantity of data, and the maximum propagation time is set to 130 days. For this trajectory segment, the center of propagation was set to the Earth-Moon L2 point. The transfer data generated from this analysis is then filtered to select the transfer segments that can be connected to a GTO with a feasible ΔV. In particular, a transfer is assumed to be valid if the inclination and argument of periapsis of its periapsis state are respectively within 20 degrees and 60 degrees of the values assumed for the GTO.

GTO Bridge Design

In general, the periapsis of the transfer leg is located in a different plane than the plane of a GTO, because both the inclination and the argument of periapsis assume different values. As such, orbital maneuvers are needed to move from the plane of the GTO to the plane of the transfer. MONTE provides a function to compute such plane changes, where two-body dynamics are used to estimate a combined maneuver that changes the inclination, longitude of the ascending node, and an optional third conic parameter from the initial orbit to the target orbit. The change in inclination and longitude of ascending node is achieved with an out-of-plane component of ΔV, while the change in the third parameter is obtained with an in-plane component of ΔV. In order to connect the GTO to the transfer trajectory, the argument of periapsis is chosen as the optional parameter, so that the plane of the GTO is effectively rotated in the direction of the transfer trajectory and the injection can be achieved with a periapsis burn. The location of the combined maneuver is found at the intersection of the two orbital planes. By defining $\Delta\Omega = \Omega_2 - \Omega_1$ as the difference in right ascension of the ascending node (RAAN) between the initial orbit and the plane of the transfer trajectory, the intersection is found using spherical geometry:

$$u_1 = \text{atan2}(-\sin i_2 \sin \Delta\Omega,\ \cos i_2 \sin i_1 - \sin i_2 \cos i_1 \cos \Delta\Omega) \tag{2}$$

$$u_2 = \text{atan2}(-\sin i_1 \sin \Delta\Omega,\ -\cos i_1 \sin i_2 + \sin i_1 \cos i_2 \cos \Delta\Omega) \tag{3}$$

where u is the argument of latitude and i is the inclination. The algorithm to find the combined maneuver between the two planes first computes the out-of-plane component of delta-V required to match the inclination and the RAAN of the target, and subsequently tries to determine the in-plane component of delta-V required to match the argument of periapsis of the target by computing the partial derivative of the target coordinate with respect to the velocity increment in the T-axis of the RTN (Radial, Transverse, Normal) frame. Since the in-plane ΔV component only exists if this partial derivative is not zero, these combined maneuvers are not possible for all combinations of orbits. Furthermore, a downside of this approach is that, for certain combination of states, the computation of the maneuver converges to a finite value, but the resulting trajectory is non-physical (e.g. the new periapsis is below the surface of the Earth); to avoid this phenomenon, the altitude of the periapsis can be iteratively increased until a valid trajectory is found. Furthermore, a phasing maneuver is required to ensure that the injection location is reached at the correct time.

As such, the design of the connecting leg is composed of the following elements:

1. An apoapsis maneuver to increase the initial periapsis altitude to at least 400 km. This is needed to reduce the impact of drag at low altitude, which could lead to the decay and hence premature ending of the orbit.

2. A combined plane change maneuver, performed at the intersection of the planes of the GTO and of the transfer trajectory, which changes the values of inclination, longitude of ascending node, and argument of periapsis of the GTO.

3. A phasing maneuver, which raises the apoapsis of the trajectory so that the injection location is reached at the correct time.

4. An injection maneuver, performed at the periapsis of the trajectory, which raises the apoapsis and puts the spacecraft on the required low-energy transfer.

The results produced by this algorithm are illustrated in Figure 1, which shows the orbital elements of the spacecraft as a function of time. The impulsive maneuvers are easily seen as abrupt changes in the plot, and it can be observed that the perturbations (drag, spherical harmonics, third body perturbations) do not significantly alter the orbital elements in the short term. In Figure 2, the trajectory resulting from the algorithm is shown in the EME2000 frame. The choice of using the argument of periapsis as the third parameter in the plane change is made to ensure that the injection maneuver can be performed at periapsis, but it can also be seen that the plane change maneuver increases the semimajor axis of the trajectory, which reduces the cost of the subsequent injection maneuver.

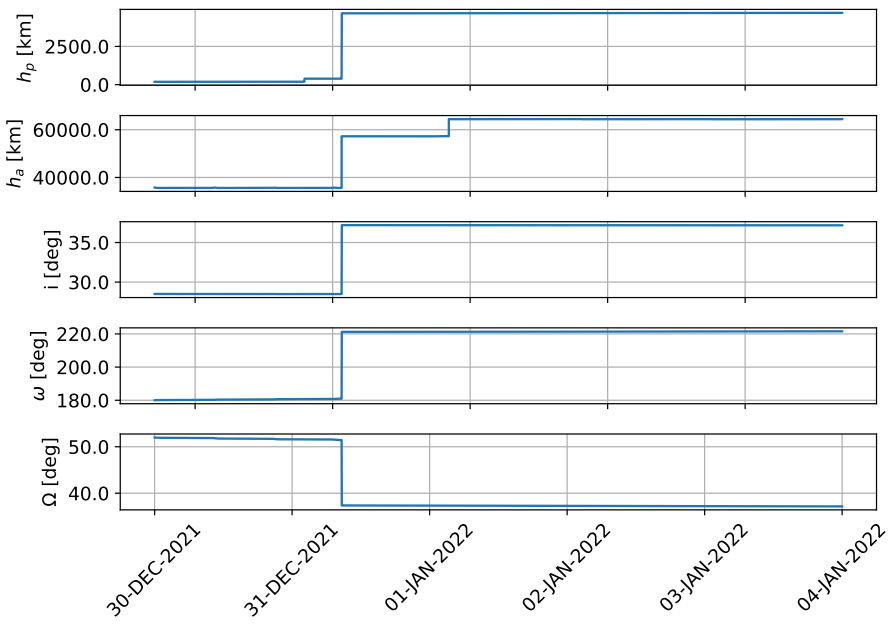

Figure 1. Orbital elements of a trajectory connecting the initial GTO to the transfer trajectory

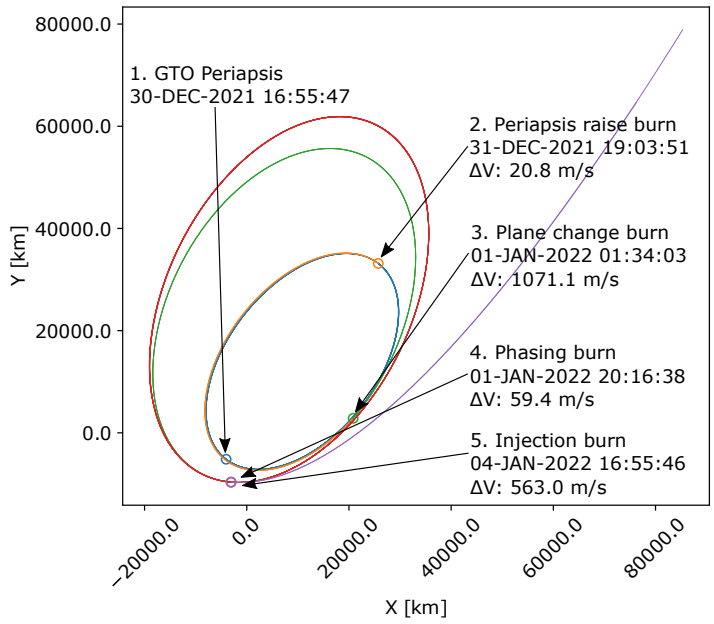

Figure 2. Maneuver sequence of trajectory connecting the initial GTO to the transfer trajectory

Trajectory Optimization

The bridge segment computed in the previous step changes the plane of the spacecraft from the initial GTO to the plane of the transfer trajectory. This puts the spacecraft in the correct geometry to reach the transfer trajectory, but the injection location of this trajectory is generally at a different altitude than the original transfer computed via backward propagation. As a result, the new trajectory follows a path similar to the original trajectory for a span of time after the injection maneuver, but it eventually diverges. Therefore, an optimization algorithm is run to compute two small impulsive maneuvers that ensure that the spacecraft arrives at the intended target orbit.

The optimization is performed using the COSMIC application available in MONTE.[10] COSMIC is designed to minimize the total ΔV of a mission by dividing the trajectory into a series of independent segments. The overall problem structure is configured by defining a time line of trajectory events. Each independent segment is associated with a single control point which defines the initial condition for the propagation forward and backward from the control point. The propagated arcs meet at break points where various continuity constraints are enforced to ensure that the resulting trajectory is smooth. The optimizer used to solve the problem is the Interior Point Optimizer (IpOpt). The optimizer is allowed to vary the control point parameters (epoch, state coordinates) and maneuver parameters (epoch, ΔV). Constraints can be applied to the control parameters and to other arbitrary functions (including trajectory parameters, burn directions, etc.). The optimization scheme is defined using the following elements:

1. A control point at the injection location of the trajectory. No controls are assigned for this point, since the injection state was computed in the previous step.
2. A trajectory correction maneuver, 20 days after departure, for which controls are assigned on the Cartesian components and epoch of the maneuver.
3. A breakpoint, located 10 days before the arrival epoch, to which a second impulse maneuver is associated. At the breakpoint, the trajectory propagated backward from the final control point must match with the trajectory propagated forward from the initial control point.
4. A control point on the stable manifold of the target libration orbit. No controls are assigned for this point, since the stable manifold naturally flows toward the target libration orbit.

In Figure 3, a comparison is shown between the trajectory obtained from the backward propagation of the initial state on the Earth-Moon Halo orbit, the trajectory resulting from the GTO connecting bridge before optimization, and the same trajectory after optimization. As mentioned above, it can be seen that the non-optimized trajectory (in blue) initially follows a path similar to the reference trajectory (dashed line) but it does not reach the target orbit. In Figure 4, the same trajectories are shown in the Earth-Moon rotating frame. Here, it can also be observed that the Halo orbit is stable for about one revolution without any additional maneuver.

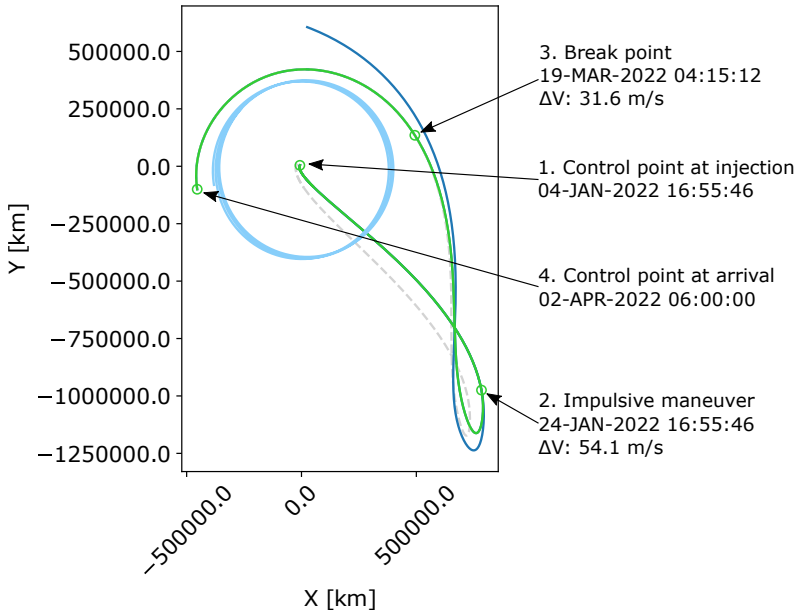

Figure 3. Comparison of the reference trajectory (dashed line), transfer trajectory before optimization (blue) and after optimization (green), shown in the Sun-Earth rotating frame

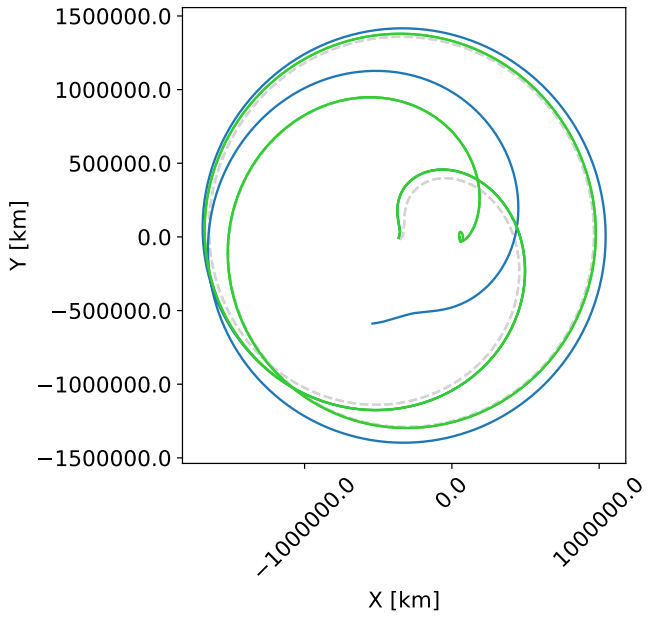

Figure 4. Comparison of the reference trajectory (dashed line), transfer trajectory before optimization (blue) and after optimization (green), shown in the Earth-Moon rotating frame

RESULTS

The low-energy transfer solutions found from the Earth-Moon L2 Halo orbit to Earth periapsis via backward propagation are shown in Figures 5(a) and 5(b). Here, the x-axis represents the injection epoch (i.e. the epoch of the Earth periapsis of the transfer trajectory), while the y-axis represents the mean local solar time of the injection location. The color of the solutions represents the time of flight of the transfer (from the injection epoch to the arrival at the Halo orbit), and it can be seen that the majority of the solutions have a time of flight between 80 and 100 days. As expected, Figure 5(a) shows repeating patterns from one synodic month to the other, which are due to the approximately repeating geometry of the Sun-Earth-Moon system. However, when filtering these solutions to select the ones which are geometrically compatible with an injection from GTO, a large number of options are removed, and the periodic pattern disappears.

In Figure 5(b), the low-energy transfer solutions that are compatible with the GTO geometry are shown. In particular, it can be seen that the solutions in the winter months are compatible with a GTO launch around midday, whereas the solutions in the summer months are compatible with a GTO launch around midnight. Overall, this shift limits the window of opportunity for a rideshare mission. Furthermore, it can be observed that a gap in the data occurs around the months of February and September, where only a small number of solutions are available.

Having determined the available transfer options, the ΔV required to inject from the initial GTO into the transfer trajectory is computed. In Figure 6, the cost of the GTO bridge as a function of the mean local solar time of the GTO is shown. The figures clearly show that the major component of the ΔV cost is due to the plane change, rather than the injection. Due to the difference between the orbital planes, the mean local solar time of the GTO with minimum ΔV is not the same as the mean local solar time of the transfer trajectory periapsis (indicated by a dashed line), but is slightly shifted. It can also be observed that the cost of the phasing maneuver has an oscillating behavior, which causes an oscillation in the injection cost (i.e. an increase to the periapsis altitude due to a phasing maneuver reduces the ΔV needed at injection, since both maneuvers are performed at periapsis). While the minimum value of the total ΔV is within the budget assumed for the spacecraft, the range of viable times for the launch is restricted to a small window, which could limit the available options for a rideshare launch.

In Figures 7(a) and 7(b), the ΔV costs for the months of January and June are shown. For each transfer solution, the solar time and ΔV of the GTO requiring the lowest ΔV are shown in the plot. From the plots, it can be observed that the ΔV requirements of the solutions for January are generally higher than the ones for June, leading to some unfeasible options. Furthermore, it can also be observed that the solar time of the GTO periapsis shifts throughout the month, so that a specific time of launch for a certain day might not be a valid solution for a day later in the month. However, solutions for midday and midnight launches are available throughout most of January and June respectively, thus giving options for the rideshare mission design.

The final optimization of the transfer leg, which is performed after the computation of the GTO bridge segment, achieves convergence in less than 50 iterations, and it was found that the average cost of the correction maneuvers for the available data is 56.1 m/s, with standard deviation of 29.5 m/s. By choosing one of the transfer solutions with a cost of 1.8 km/s or lower, the ΔV budget available for the spacecraft is sufficient for reaching the target Halo orbit and leaves residual ΔV which can be used for station-keeping once the Halo orbit is achieved.

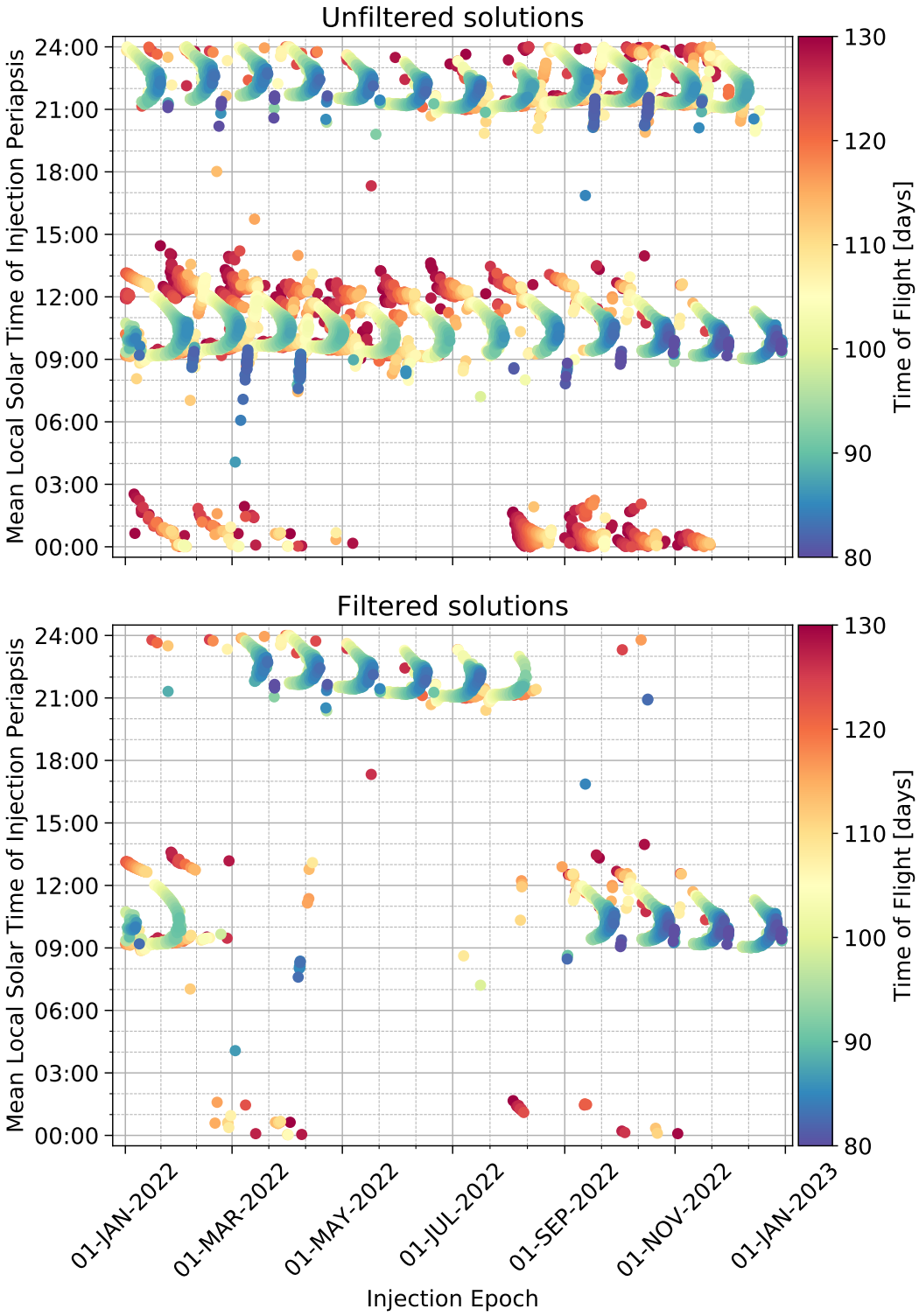

Figure 5. Low-energy transfers to the target L2 Halo orbit.
(a) Global solutions (b) Solutions compatible with a GTO at 28.5° inclination

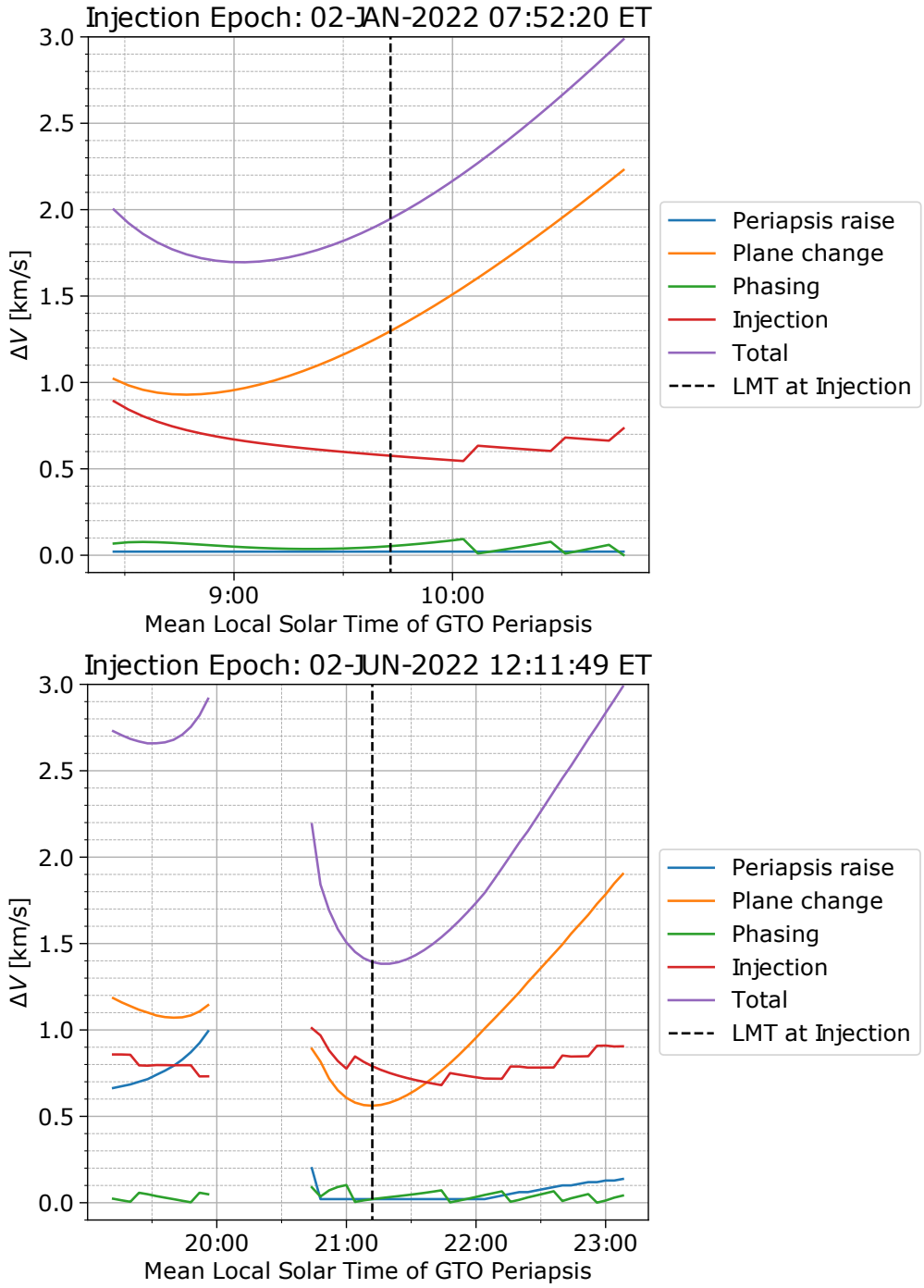

Figure 6. Cost of the GTO bridge trajectory for two launch options (a) Near-midday launch (b) Near-midnight launch

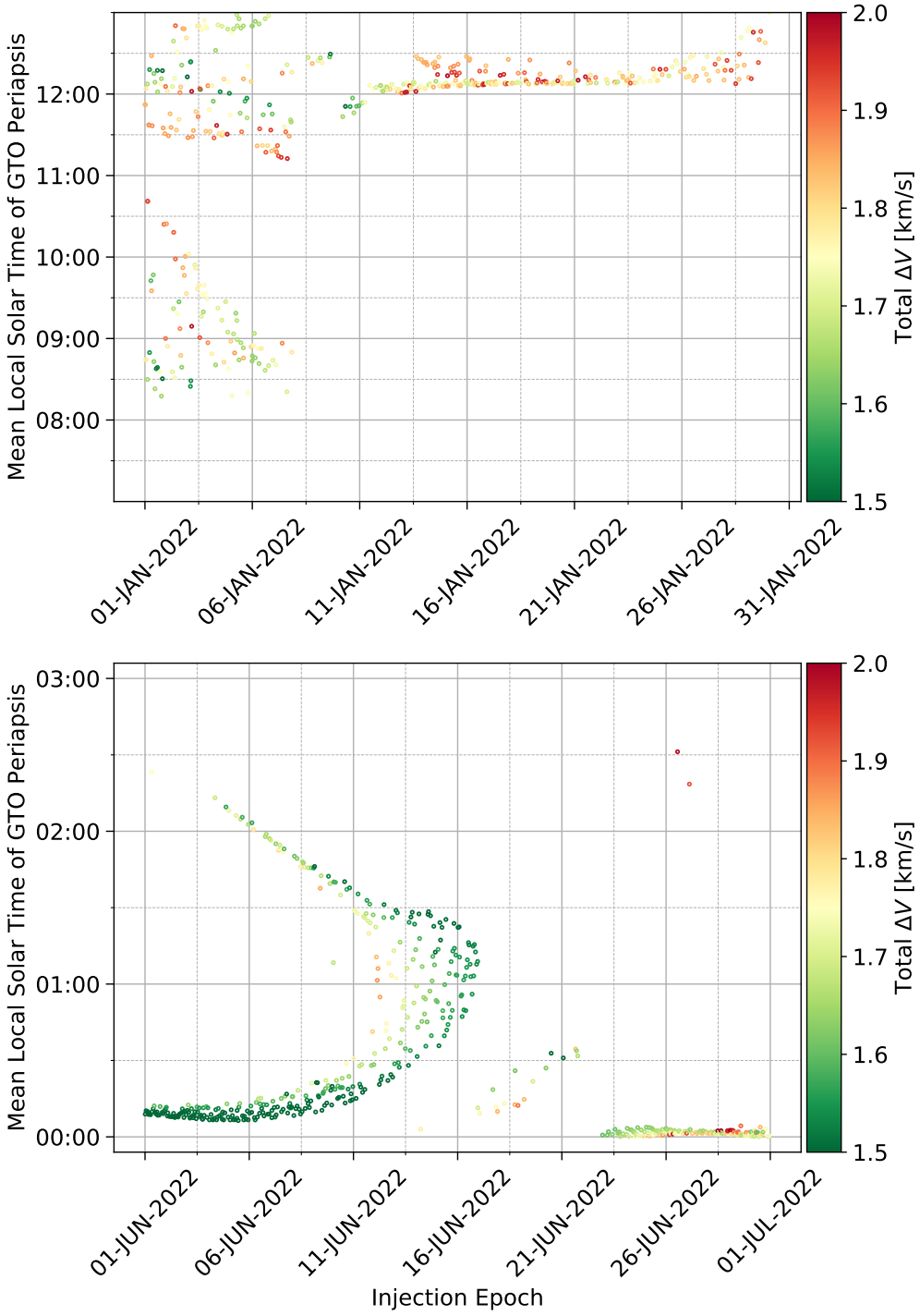

Figure 7. ΔV **of GTO to Earth-Moon L2 Halo transfers**
(a) January launches (b) June launches

CONCLUSIONS

This investigation shows the feasibility of a rideshare mission from a geosynchronous transfer orbit to a lunar libration orbit using the methodology presented here. In particular, transfer solutions can be found throughout the entire year (although a shift in the launch time occurs from the winter months to the summer months) and the required ΔV budget is within the capabilities assumed for the spacecraft.

There are two possible routes to improve on the results presented in this paper, which will be the focus of future work. The first element that requires further work is the GTO bridge segment. This trajectory segment is generated by estimating the required maneuvers using two-body dynamics, but no optimization is performed. A preliminary analysis has shown that optimizing the parameters of the maneuvers can reduce the cost of this segment by 100 - 200 m/s. Such large savings would increase the payload mass to the target orbit and ensure that all the transfer solutions found are feasible, giving more freedom in the design of a mission. Additionally, the whole end-to-end trajectory could also be optimized, allowing the injection state and epoch and the arrival state and epoch to vary.

Secondly, further improvements can be achieved by incorporating low-thrust propulsion into the problem. Low-thrust is a more realistic option for a smallsat, considering the fact that a smallsat can only achieve a limited level of thrust, and can help in increasing the payload mass delivered to the target orbit. The development of a trajectory design methodology that leverages low-thrust propulsion will significantly increase the difficulty of the problem, but the results presented in this investigation can be used as a first guess to compute the low-thrust trajectories.

ACKNOWLEDGEMENTS

This research was carried out at the Jet Propulsion Laboratory, California Institute of Technology, and was sponsored by the JPL Visiting Student Research Program (JVSRP) and the National Aeronautics and Space Administration (80NM0018D0004).

REFERENCES

[1] H. Pernicka, D. Scarberry, S. Marsh, and T. Sweetser, "A search for low Delta-V Earth-to-Moon trajectories," *Astrodynamics Conference*, American Institute of Aeronautics and Astronautics, Aug. 1994, 10.2514/6.1994-3772.

[2] A. L. Genova, F. Y. Yang, A. D. Perez, K. F. Galal, N. T. Faber, S. Mitchell, B. Landin, A. Datta, and J. O. Burns, "Trajectory Design From GTO To Lunar Equatorial Orbit For The Dark Ages Radio Explorer (DARE) Spacecraft," 2015.

[3] W. Koon, M. Lo, J. Marsden, and S. Ross, "Low Energy Transfer to the Moon," *Celestial Mechanics and Dynamical Astronomy*, Vol. 81, Sep 2001, 10.1023/A:1013359120468.

[4] G. Mingotti and F. Topputo, "Ways to the Moon: A survey," *Advances in the Astronautical Sciences*, Vol. 140, 01 2011, pp. 2531–2547.

[5] J. A. O. Romero and K. C. Howell, "Transfers from GTO to Sun-Earth libration orbits," *Advances in the Astronautical Sciences*, 2019.

[6] D. Folta, D. J. Dichmann, P. Clark, A. Haapala, and K. Howell, "Lunar cube transfer trajectory options," *Advances in the Astronautical Sciences*, 2015.

[7] D. Quantius, J. Spurmann, E. Dekens, and H. Päsler, "Weak Stability Boundary Transfer to the Moon Launched Piggy-Back on Ariane 5 to GTO," *Deutscher Luft- und Raumfahrtkongress*, 09 2011.

[8] E. Taheri and J. L. Junkins, "How Many Impulses Redux," *The Journal of the Astronautical Sciences*, Vol. 67, Dec. 2019, pp. 257–334, 10.1007/s40295-019-00203-1.

[9] E. T. Sandeep K. Singh, Brian D. Anderson and J. L. Junkins, "Exploiting Manifolds of Halo Orbits for End-to-End Earth-Moon Low-Thrust Trajectory Design," *Celestial Mechanics and Dynamical Astronomy*, Feb 2020.

[10] S. Evans, W. Taber, T. Drain, J. Smith, H.-C. Wu, M. Guevara, R. Sunseri, and J. Evans, "MONTE: the next generation of mission design and navigation software," *CEAS Space Journal*, Vol. 10, 01 2018, 10.1007/s12567-017-0171-7.

[11] V. Szebehely, *Theory of Orbits*. New York City, New York, USA: Academic Press, 1967.

[12] J. Parker, "Low-energy ballistic lunar transfers," *The Journal of the Astronautical Sciences*, Vol. 58, July 2011, 10.1007/BF03321173.

[13] Bruinsma, Sean, "The DTM-2013 thermosphere model," *Journal of Space Weather and Space Climate*, Vol. 5, 2015, p. A1, 10.1051/swsc/2015001.